



HAL
open science

Application of MALDI-TOF MS to species complex differentiation and strain typing of food related fungi: Case studies with *Aspergillus* section *Flavi* species and *Penicillium roqueforti* isolates

Laura Quéro, Priscillia Courault, Beatrice Cellière, Sophie Lorber, Jean-Luc Jany, Olivier Puel, Victoria Girard, Valérie Vasseur, Patrice Nodet, Jerome Mounier

► To cite this version:

Laura Quéro, Priscillia Courault, Beatrice Cellière, Sophie Lorber, Jean-Luc Jany, et al.. Application of MALDI-TOF MS to species complex differentiation and strain typing of food related fungi: Case studies with *Aspergillus* section *Flavi* species and *Penicillium roqueforti* isolates. *Food Microbiology*, 2020, 86, pp.103311. 10.1016/j.fm.2019.103311 . hal-02271931

HAL Id: hal-02271931

<https://hal.science/hal-02271931>

Submitted on 20 Jul 2022

HAL is a multi-disciplinary open access archive for the deposit and dissemination of scientific research documents, whether they are published or not. The documents may come from teaching and research institutions in France or abroad, or from public or private research centers.

L'archive ouverte pluridisciplinaire **HAL**, est destinée au dépôt et à la diffusion de documents scientifiques de niveau recherche, publiés ou non, émanant des établissements d'enseignement et de recherche français ou étrangers, des laboratoires publics ou privés.



Distributed under a Creative Commons Attribution - NonCommercial 4.0 International License

1 **Application of MALDI-TOF MS to species complex differentiation and strain typing of**
2 **food related fungi: case studies with *Aspergillus* section *Flavi* species and *Penicillium***
3 ***roqueforti* isolates**

4
5 Laura Quéro^{a,b}, Priscillia Courault^b, Beatrice Cellière^b, Sophie Lorber^c, Jean-Luc Jany^a,
6 Olivier Puel^c, Victoria Girard^b, Valérie Vasseur^a, Patrice Nodet^a, Jérôme Mounier^{a*}

7
8 ^aUniv Brest, Laboratoire Universitaire de Biodiversité et Ecologie Microbienne, F-29280
9 Plouzané, France.

10
11 ^bbioMérieux, R&D Microbiologie, route de Port Michaud, 38390 La Balme les Grottes,
12 France.

13
14 ^cToxalim (Research Center in Food Toxicology), Université de Toulouse, INRA, ENVT,
15 INP-Purpan, UPS, 31027 Toulouse

16
17 Laura Quéro : laura.queo@univ-brest.fr

18 Priscillia Courault : priscillia.courault@biomerieux.com

19 Béatrice Cellière : beatrice.celliere@biomerieux.com

20 Sophie Lorber : sophie.lorber@inra.fr

21 Jean-Luc Jany : jean-luc.jany@univ-brest.fr

22 Olivier Puel : olivier.puel@inra.fr

23 Victoria Girard : victoria.girard@biomerieux.com

24 Valérie Vasseur : valerie.vasseur@univ-brest.fr

25 Patrice Nodet : patrice.nodet@univ-brest.fr

26 Jérôme Mounier : jerome.mounier@univ-brest.fr

27
28 ***Corresponding author:** Jérôme Mounier, Laboratoire Universitaire de Biodiversité et Ecologie Microbienne,
29 Parvis Blaise-Pascal, Technopôle Brest-Iroise, 29280 Plouzané, France, Tel: +33 (0)2.90.91.51.00, Fax: +33
30 (0)2.90.91.51.01

31 E-mail: jerome.mounier@univ-brest.fr.

32

33 **Abstract**

34 Filamentous fungi are one of the main causes of food losses worldwide and their ability to
35 produce mycotoxins represents a hazard for human health. Their correct and rapid
36 identification is thus crucial to manage food safety. In recent years, MALDI-TOF emerged as
37 a rapid and reliable tool for fungi identification and was applied to typing of bacteria and
38 yeasts, but few studies focused on filamentous fungal species complex differentiation and
39 typing. Therefore, the aim of this study was to evaluate the use of MALDI-TOF to identify
40 species of the *Aspergillus* section *Flavi*, and to differentiate *Penicillium roqueforti* isolates
41 from three distinct genetic populations. Spectra were acquired from 23 *Aspergillus* species
42 and integrated into a database for which cross-validation led to more than 99% of correctly
43 attributed spectra. For *P. roqueforti*, spectra were acquired from 63 strains and a two-step
44 calibration procedure was applied before database construction. Cross-validation and external
45 validation respectively led to 94% and 95% of spectra attributed to the right population.
46 Results obtained here suggested very good agreement between spectral and genetic data
47 analysis for both *Aspergillus* species and *P. roqueforti*, demonstrating MALDI-TOF
48 applicability as a fast and easy alternative to molecular techniques for species complex
49 differentiation and strain typing of filamentous fungi.

50

51 **Keywords** : MALDI-TOF MS ; filamentous fungi ; species complex ; strain typing

52

53 **1. Introduction**

54

55 Fungi are frequently involved in food spoilage and represent a major cause of food and
56 economic losses. Indeed, among food losses and waste which represent 1 billion tons each
57 year (FAO, 2011), it is estimated that 5 to 10% of them are due to fungal spoilage
58 (Filtenborg, Frisvad, and Thrane 1996; Pitt and Hocking 2009). Fungi can spoil a large
59 variety of feeds and foods, causing organoleptic properties deterioration such as visible
60 growth on the product surface, off-flavor production, texture and color changes. Moreover, a
61 large number of species such as *Penicillium* and *Aspergillus* spp. are potential mycotoxin
62 producers, and may represent a great hazard for human health (Waśkiewicz 2014). Hence,
63 rapid and reliable identification of filamentous fungi is a key step for a better management of
64 food safety and quality.

65 For several years now, MALDI-TOF MS has been successfully applied to microorganism
66 identification, from bacteria (Basile et al. 1998) to fungi (Welham et al. 2000) including

67 food-related fungi (Quéro et al. 2018). In the latter study, a spectral database comprising 619
68 strains belonging to 136 species of food interest was built and 90 % correct identification at
69 the species level were achieved after external validation. Several commercial instruments and
70 databases are available (Deak et al. 2015) for routine identification. Besides identification at
71 species level, MALDI-TOF MS has been shown as a powerful tool to discriminate fungal
72 species complex and cryptic fungal species. As an example, Al-Hatmi et al. (2015) were able
73 to correctly identify species of clinical interest belonging to the *Fusarium fujikuroi* complex,
74 some of which being cryptic species. Allen et al. (2005) defined species complex as a cluster
75 of related isolates which individuals may represent more than one species while cryptic
76 species are morphologically indiscernible biological/phylogenetic units that are only revealed
77 using DNA-based molecular analysis (Hawksworth 2006). In most cases, the identification of
78 such species requires the analysis of several specific genes and expertise in data analysis
79 (Balasundaram et al. 2015). Species complex are an issue not only in clinical context but also
80 in the food context, particularly regarding mycotoxin production. For example, in the
81 *Aspergillus* genera, and more particularly in the *Flavi* section which contains several cryptic
82 species and currently comprises 33 phylogenetically distinct species (Frisvad et al. 2019),
83 species have different mycotoxin production abilities, some species being able to produce B1,
84 B2, G1 and G2 aflatoxins (e.g. *A. nomius*, *A. novoparasiticus*, *A. parasiticus*) while others
85 only produce B1 and B2 aflatoxins (*A. flavus*, *A. pseudotamarii* and *A. togoensis*) or no
86 aflatoxins (*A. caelatus*, *A. subflavus* and *A. tamarii*) (Frisvad et al. 2019). Another challenge
87 within this section is the discrimination between the toxigenic *Aspergillus flavus* and *A.*
88 *parasiticus* and the non-toxigenic *A. oryzae* and *A. sojae*, the latter being used in the
89 production of numerous fermented products like sake or soy sauce (Gibbons et al. 2012).
90 In order to discriminate *Aspergillus* species, MALDI-TOF MS could be a good alternative to
91 molecular techniques, because of its accuracy, high-throughput and low cost per analysis.
92 Several studies already pointed out its use for different *Aspergillus* sections including the
93 *Flavi* section. For example, Alanio et al. (2011) used MALDI-TOF MS for discriminating 10
94 species of *Aspergillus* section *Fumigati* while Hettick et al. (2008) and De Carolis et al.
95 (2012) could differentiate *A. flavus* from *A. parasiticus*, and *A. parasiticus*, *A. flavus* and *A.*
96 *oryzae*, respectively. In a more extensive study, Rodrigues et al. (2011) could identify 9
97 species of *Aspergillus* section *Flavi* but could not distinguish aflatoxigenic and non-
98 aflatoxigenic isolates of *A. Flavus*. More recently, Imbert et al. (2019) assessed MALDI-TOF
99 MS identification accuracy of *Aspergillus* cryptic species on a very large dataset of 1477
100 isolates using the freely available mass spectrometry identification (MSI) platform. After

101 sequencing a subset of 245 cryptic species isolates for confirmation, they showed that, while
102 very good identification (99.6 %) could be achieved with MALDI-TOF MS at the section
103 level, only 66.1% of isolates were correctly assigned at the species level indicating that the
104 database needed further improvement for cryptic species.

105

106 To another extent, MALDI-TOF MS could also be of great interest for differentiating strains
107 from a same species, i.e. for strain typing. In the past 10 years, it has been applied to bacteria
108 of different genera and species such as *Salmonella enterica* (Kuhns et al. 2012),
109 *Staphylococcus aureus* (Ueda et al. 2015), *Legionella* spp. (Fujinami et al. 2011) or
110 *Arthrobacter* spp. (Vargha et al. 2006) and could be in some cases as effective as traditional
111 typing methods such as multi-locus sequence typing (MLST) or Pulsed-Field Gel
112 Electrophoresis (PFGE). In a recent study, Kern et al. (2014) showed the ability of MALDI
113 TOF MS to differentiate *Lactobacillus brevis* isolates at the strain level, and correlations
114 could also be made between spectra classification and strain physiological properties.
115 MALDI-TOF MS typing was also applied to yeasts of clinical interest, for which it could be
116 as powerful as microsatellite markers for monitoring the spread of nosocomial infections
117 (Pulcrano et al. 2012). This technique was also recently applied for the typing of brewing
118 yeast strains allowing their classification into different major beer types (Lauterbach et al.
119 2017) as well as for the typing of 33 wine yeasts which could be sorted according to their
120 genetic background (Usbeck et al. 2014). One of the main challenges of fungal typing is that,
121 as compared to bacteria, their phylogenetic relationships are more complex and species
122 boundaries are not easily drawn (Bader 2013). Nevertheless, a rapid and reliable method for
123 fungal typing would be of great interest in several contexts, *e.g.*, to help understanding the
124 domestication process and history of numerous species used in industry, for source-tracking
125 of spoilage fungi in the food industry, to differentiate toxigenic and atoxigenic strains of a
126 same species, to discriminate the different strains involved in natural fermentation processes
127 for the selection of starter cultures and for deciphering the tenuous limits between
128 contaminant and biotechnological isolates (Belén Flórez et al. 2007). In the past 15 years,
129 several studies focused on strain-level classification of filamentous fungi with technological
130 interest such as those used in cheese manufacture. Belén Flórez et al. (2007) and Fontaine et
131 al. (2015), using randomly amplified polymorphic DNA (RAPD)-PCR, could discriminate, at
132 the intraspecies level, *P. roqueforti* isolates from cheese and environmental origins.
133 Microsatellite markers were also used to investigate the genetic diversity within *Penicillium*
134 *roqueforti* isolates (Ropars et al. 2014; Gillot et al. 2015), and these studies allowed the

135 differentiation of isolates in several genetically divergent populations. For instance, Gillot et
136 al. (2015), using 4 polymorphic microsatellite markers, distinguished 28 haplotypes among a
137 worldwide collection of 164 *P. roqueforti* isolates from cheese and other environments.
138 Furthermore, these 28 haplotypes could be clustered into three well-defined genetically
139 differentiated populations.

140 While there is a strong body of evidence that MALDI-TOF MS can be applied to
141 discriminate closely-related bacterial species and bacterial strains, only few studies have
142 evaluated MALDI-TOF MS as a rapid tool to differentiate closely-related fungal species and
143 strains or genetic populations from a same species. Therefore, the aim of this study was first
144 to evaluate the potential of MALDI-TOF MS to accurately identify 23 closely-related
145 species of *Aspergillus* section *Flavi*, and then to assess whether this technique could be used
146 for discriminating *Penicillium roqueforti* isolates previously shown by Gillot et al. (2015) to
147 belong to three distinct genetic populations.

148

149 **2. Materials and methods**

150

151 **2.1 Fungal strains and cultivation**

152

153 Sixty-eight strains belonging to 23 species from the *Aspergillus* section *Flavi* were obtained
154 from different culture collections. They are listed in Table 1. Strain identification was
155 performed by DNA sequencing in previous studies (Frisvad et al. 2019 ; Carvajal-Campos et
156 al. 2017 ; Quéro et al. 2018) or by the culture collection providing the isolates. Sixty-three
157 *Penicillium roqueforti* isolates obtained from the Université de Bretagne Occidentale Culture
158 Collection (UBOCC), Centraalbureau voor Schimmelcultures (CBS), Mycology laboratory of
159 the Institute of Hygiene and Epidemiology (IHEM), Mycothèque de l'Université Catholique
160 de Louvain (MUCL), Deutsche Sammlung von Mikroorganismen und Zellkulturen (DSMZ),
161 and Laboratoire Cryptogamie Paris (LCP) collections belonging to 28 haplotypes and
162 classified into three genetically distinct populations (1, 2 and 3) were chosen among the 164
163 isolates which were studied by Gillot et al. (2015). Twenty-one, 22 and 20 isolates belonged
164 to population 1, 2 and 3, respectively (Supplementary Table 1).

165

166 To assess viability and purity before spectra acquisition, all strains were first cultivated at
167 25°C on Malt Extract Agar (20 g.L⁻¹ malt extract, 3 g.L⁻¹ yeast extract, 15 g.L⁻¹ agar) and
168 Potato Dextrose Agar (PDA, bioMérieux, Marcy l'Etoile, France), for *Aspergillus* spp. and *P.*

169 *roqueforti*, respectively. Then, they were cultivated on their respective media for 8 days at
170 25°C before spectra acquisition. Three culture replicates were made for each strain.

171

172 **2.2 Sample preparation and spectra acquisition**

173

174 After cultivation, isolates were processed following the manufacturer's instructions
175 (bioMérieux, Marcy l'Etoile, France) as described previously (Quéro et al. 2018). Briefly,
176 fungal biomass was suspended in 70% ethanol, before formic acid/acetonitrile protein
177 extraction and centrifugation. After samples and matrix were deposited on target slides,
178 spectra were acquired using the VITEK MS system (bioMérieux, Marcy l'Etoile, France)
179 equipped with the Launchpad V2.8.4 acquisition software. Each sample was analyzed in
180 duplicate.

181 All spectra were acquired in linear positive ion extraction mode in a mass range from 2000 to
182 20,000 Da. Individual spectra were accumulated from 500 laser shots (100 profiles with 5
183 shots per profile) with the 'Auto-Quality' option activated. The system was calibrated
184 externally with fresh cells of *Escherichia coli* ATCC 8739. Raw spectra were automatically
185 processed by smoothing and peak detection procedures implemented in the Launchpad
186 acquisition software (bioMérieux, Marcy l'Etoile, France).

187 Raw spectra were then controlled for peak resolution, signal-to-noise ratio and absolute
188 signal intensity as described previously (Girard et al. 2016). The spectra that did not reach the
189 specified quality criteria were discarded.

190

191 **2.3 Discrimination of *Aspergillus* section *Flavi* species complex**

192

193 Two approaches were used to evaluate the power of MALDI-TOF MS to discriminate
194 *Aspergillus* species from the *Flavi* section. First, a non-supervised approach was used in
195 which the distances between all spectra were determined using the classical multidimensional
196 scaling function (cmdscale) of Matlab (2014, The Mathworks Inc., USA). The calculated
197 distances between spectra were based on the absence or presence of peaks and their
198 intensities. These distances were then visualized using a multidimensional scaling (MDS)
199 graphic. Secondly, a supervised approach was used after building a spectral database with 61
200 strains as previously described (Girard et al. 2016; Quéro et al. 2018). Briefly, peak lists were
201 binned and a predictive model was established using the Advanced Spectra Classifier (ASC)
202 algorithm developed by bioMerieux (Marcy l'Etoile, France). Briefly, the ASC algorithm

203 assigns weights to each bin depending on the absence or presence of a peak. For example, if a
204 peak is always present in a bin for spectra of population 1 and absent in the same bin for the
205 other groups, the algorithm will assign a high positive weight to that bin for classification of
206 unknown spectra. On the contrary, if a peak is always absent for population 1 and present in
207 the other populations, it will have a high negative weight. Moreover, if a peak is either
208 present or absent in spectra of the same population, it will have a low weight as it is poorly
209 discriminant. This decision algorithm was applied to only retain significant matches and a
210 single choice identification was obtained when only one species was retained. When more
211 than one species was retained, a low discrimination result was proposed. In case more than 4
212 species were retained or if no significant match was found, it was considered as a non-
213 identification result.

214 Spectra acquired from 7 species, i.e., *A. bertholletius*, *A. coremiiformis*, *A. cerealis* (ex *A.*
215 *korhogoensis*), *A. mottae*, *A. oryzae*, *A. pseudocaelatus* and *A. pseudonomius* were not
216 included in the database as the number of tested strains was not sufficient. Indeed, the ASC
217 algorithm used for database construction requires a minimum of 2 strains per species.
218 Performances of this database were then evaluated using the same set of isolates by cross-
219 validation, i.e., internal validation, as described previously (Quero et al. 2018). The spectral
220 data were randomly split into 5 subsets, 4 subsets used as learning phase and the last one used
221 to validate the identification performances (or in this case, the attribution to the right group).
222 This procedure was repeated 5 times, each subset being used once as a test. A correct
223 identification was defined when the same identification occurred between cross-validation
224 result and the reference identification. Low discrimination results were considered as correct
225 if the expected identification was included in the matches. A misidentification result was
226 defined as a discordant identification between the cross-validation result and the reference
227 identification.

228

229

230 **2.4 Discrimination of *Penicillium roqueforti* isolates**

231

232 Prior to similarity comparison of spectra and database construction, a two-step calibration
233 was applied on all spectra, involving a linear calibration step to correct any possible global
234 mass shift and a quadratic calibration step on the spectra entire mass range.

235 For linear calibration, specific MS peaks of *P. roqueforti* spectra were used. To do so, MS
236 spectra of *P. roqueforti* isolates recorded in the bioMérieux commercial database (version
237 3.2) were screened for specific MS peaks, which were then searched in the spectra acquired
238 in the present study. Thirteen specific MS peaks with masses ranging from 3704.84 to
239 14431.15 Da were found. Then, only MS peaks present in more than 70% of isolates
240 belonging to two of the three genetic populations were kept which led to the selection of 9
241 MS peaks with a mass of 3704.84, 3746.12, 4972.23, 6242.47, 6777.90, 6840.56, 7409.58,
242 7437.67 and 14431.14 Da. The selected theoretical MS peaks were then compared to those
243 observed in the spectra acquired in the present study, allowing the application of a linear
244 model to correct eventual mass deviations. After mass correction with linear calibration, a
245 quadratic calibration was applied. For this calibration step, the entire mass range (3000-20000
246 Da) was targeted, in which masses ranging between 3000 and 6000 Da, 6000 and 10000 Da
247 and 10000 and 20000 Da were screened using a 1-,2- and 3-Da interval, respectively. The
248 masse range 2000-3000 Da was excluded for quadratic calibration as it contained a very high
249 number of peaks which could bias the model used for calibration. For quadratic calibration,
250 mass tolerance was more restrictive than previously and only MS peaks present in more than
251 83% of isolates belonging to two of the three genetic populations were kept. These selected
252 masses which included 42 MS peaks (data not shown) were then used to build a quadratic
253 model between theoretical and observed masses, allowing a good alignment of spectra.

254

255 A spectral database in which the spectra derived from *P. roqueforti* isolates were assigned to
256 one of the three genetic populations identified by Gillot et al. (2015) was then implemented,
257 using the ASC algorithm.

258 Performances of this database were first evaluated by cross-validation as described above and
259 database performances were also evaluated by external validation using 21 strains not used to
260 build the database. Spectra derived from these strains were used to challenge the database to
261 assess whether they could be correctly assigned to the correct genetic population.

262

263

264 3. Results and discussion

265

266 3.1 Evaluation of MALDI-TOF MS for discriminating *Aspergillus* section *Flavi* species

267

268 The distances between spectra of all tested species can be visualized in Figure 1, which
269 shows the results of MDS analysis for all spectra (Figure 1A), spectra of the *A. flavus*-clade
270 (Figure 1B) and spectra from the other clades (Figure 1C). Overall, most species were quite
271 well separated from the others while some did not (Figure 1A). Based on spectra similarity, 3
272 groups of species could be distinguished except for spectra of *A. pseudotamarii* which stood
273 apart from these groups (Figure 1A). The first two groups (groups A and B, Figure 1A)
274 contained spectra of all species of the *A. flavus*-clade that gathers the *A. flavus* and *A.*
275 *parasiticus* related species (Varga et al, 2011) with the exception of *A. mottae* and *A. oryzae*
276 as well as spectra from *A. pseudonomius* and *A. avenaceus* from the *nomius*- and *avenaceus*-
277 clade. Although *A. mottae* is considered to belong to *A. flavus*-clade, this latter species is
278 considered as an ancestral taxon of the group including the *A. parasiticus*- and *A. flavus*-
279 subclades (Soares et a, 2012; Carvajal-Campos et al. 2017). Interestingly, Group B contained
280 all species that are closely phylogenetically related to *A. parasiticus*, namely *A. arachidicola*,
281 *A. novoparasiticus*, *A. transmontanensis*, *A. sojae* and *A. sergii*. All of these species are
282 considered in the literature as pertaining to the *A. parasiticus*-clade (Rodrigues et al. 2011;
283 Carvajal-Campos et al. 2017). It is worth mentioning that the separate grouping of *A.*
284 *parasiticus*-clade MALDI-TOF MS spectra from other *A. flavus*-clade species was also
285 reported by Rodrigues et al. (2011) but on a smaller number of species. Group C contained all
286 the species from the other clades, with the exception of *A. oryzae* and *A. mottae* from the *A.*
287 *flavus*-clade.

288 When only representing spectra from species of the *A. flavus*-clade (Figure 1B), it can be
289 observed that most of these species were clearly separated. Interestingly, spectra of *A. flavus*
290 and *A. oryzae* (the likely domesticated form of *A. flavus*) clearly stood apart despite their very
291 close phylogenetic relatedness (Frisvad et al. 2019), reflecting the fact that *A. oryzae*
292 expressed many proteins that differed from those of *A. flavus*. Indeed, it is well established
293 that domestication of *A. flavus* has led to important genetic and functional changes in its
294 metabolism (Gibbons et al. 2012). Instead, spectra of *A. oryzae* were more similar to those of
295 *A. minisclerotigenes* which is also closely phylogenetically related to *A. oryzae* (Frisvad et
296 al., 2019). In contrast to *A. flavus* and *A. oryzae*, spectra profiles of *A. parasiticus* and its
297 likely domesticated form, *A. sojae*, shared much more common characteristics. Figure 1C

298 shows the distance between spectra of the 11 other tested species belonging to the other
299 clades of *Aspergillus* section *Flavi*. Spectra of species from the *A. tamarii*-clade were
300 completely separated from the other ones but not grouped together. Indeed, spectra of *A.*
301 *tamarii* and *A. pseudotamarii* were clearly separated from each other while those of *A.*
302 *caelatus* and *A. pseudocaelatus* were more similar. Though they belonged to different clades,
303 spectra of the remaining species were grouped together except those of *A. pseudonomius* and
304 *A. avenaceus* isolates which were grouped together. Overall, spectra of the tested species
305 were quite well separated, indicating that it should be possible to differentiate and identify
306 them using a supervised approach.

307 Spectra of the 16 species which were represented by at least two strains were integrated into
308 the bioMérieux spectral database and identification performances were assessed by cross-
309 validation (Table 2). Overall, more than 99% of spectra (271/272) were assigned to the
310 correct species. Only one spectrum of *A. novoparasiticus* was not identified, and one
311 spectrum of *A. avenaceus* was attributed to both *A. avenaceus* and *A. flavus*. These results
312 show that, even if the species of *Aspergillus* section *Flavi* tested here are closely related, their
313 spectra are sufficiently different to yield correct identification when implemented into a
314 spectral database and analyzed with the ASC algorithm. Results obtained here are of
315 particular interest, especially for *A. parasiticus* and *A. sojae* whose spectra were perfectly
316 separated and identified during cross-validation. It should be noted that these species are very
317 similar from a morphological point of view; cannot be distinguished from each other based
318 only on gene sequencing of taxonomic markers such as β -tubulin, calmodulin and RPB2
319 genes and extrolite analysis is necessary to differentiate them (i.e., in contrast to *A.*
320 *parasiticus*, *A. sojae* does not produce aflatoxins and aflatrems (Frisvad et al. 2019). In the
321 same way, *A. parasiticus* and *A. novoparasiticus* were shown to share similar β -tubulin
322 sequences, requiring the sequencing of other specific genes for identification (Frisvad et al.
323 2019), whereas the analysis of their MS spectra was enough to discriminate them. This
324 analysis also allowed separation of aflatoxin-producing species (*A. aflatoxiformans*, *A.*
325 *arachidicola*, *A. flavus*, *A. luteovirescens* (ex *A. bombycis*), *A. minisclerotigenes*, *A. nomius*,
326 *A. novoparasiticus*, *A. parasiticus*, *A. pseudotamarii*, *A. sergii*, *A. transmontanensis*) from
327 non-aflatoxin producing ones (*A. avenaceus*, *A. caelatus*, *A. leporis*, *A. sojae*, *A. tamarii*). To
328 our best knowledge, this is the first time that as many species of the *Flavi* section are studied
329 and correctly identified by MALDI-TOF MS analysis. Indeed, several papers focused on the
330 identification of *Aspergillus* section *Flavi* species of clinical interest such as *A. flavus*, *A.*
331 *oryzae*, *A. nomius* or *A. tamarii* and though a separate clustering of species was obtained

332 using hierarchical analysis, no commercial databases were able to accurately identify them
333 (De Carolis et al. 2012; Li et al. 2017; Masih et al. 2016; Park et al. 2017; Rodrigues et al.
334 2011; Tam et al. 2014). This underlines the need of expanding spectral databases to reach
335 good identification performances.

336 Regarding the results obtained in the present study, MALDI-TOF MS spectra analysis could
337 be as powerful as the polyphasic approach commonly used to identify *Aspergillus* species of
338 this section which may include morphological, physiological, molecular and/or extrolite data
339 analysis (Frisvad et al., 2019, Carvajal-Campos et al, 2018). These results are very promising
340 even though they are based on a relatively low number of isolates and spectra and that only
341 16 species among the 33 currently recognized species were included in the database for
342 validation. The next step would be to integrate more species and isolates to the database as it
343 can influence identification performances (Normand et al., 2013) and also to challenge the
344 database with external isolates, in order to assess if spectra and isolates that were not used to
345 build the database can be correctly identified.

346

347 **3.2 Evaluation of MALDI-TOF MS for typing of *P. roqueforti* isolates**

348

349 **3.2.1 Similarity comparison and effect of calibration on the grouping of *P. roqueforti*** 350 **isolates**

351

352 The distances between all spectra according to their genetic populations and the impact of
353 calibration on the separation of these three populations can be visualized in Figure 2 which
354 shows the results of MDS analysis before (Figure 2A) and after calibration (Figure 2B).
355 Overall, there was a good separation of *P. roqueforti* MS spectra according to their respective
356 genetic population and the two-step calibration approach applied in the present study
357 improved separation of these spectra, thus confirming the potential of MALDI-TOF MS to
358 discriminate filamentous fungi at the intraspecific level when combined with recalibration.
359 Indeed, *P. roqueforti* isolates from population 2 were clearly separated from those of
360 populations 3 and 1 (Figure 2B), even though, for the latter population, spectra from few
361 strains, e.g., strain F77-1 which belonged to population 1, showed a high similarity with other
362 spectra from population 2. It is also worth mentioning that spectra derived from population 2
363 isolates, in contrast to population 1 and 3 spectra, showed a high heterogeneity, as underlined
364 by the distances between spectra of population 2 isolates. It was especially true for spectra
365 derived from strain F41-4 that formed a separated group from other population 2 isolates. A

366 higher genetic diversity was also reported in isolates from this population as compared to
367 other populations in the study of Gillot et al. (2015), which confirms the results obtained
368 here. Indeed, population 2 contained almost all non-cheese isolates which harbored a larger
369 number of allelic profiles to that of cheese isolates (Gillot et al. 2015). Moreover, cheese
370 isolates from this population were systematically retrieved from a given Protected
371 Designation of Origin (PDO) or Protected Geographical Indication (PGI) cheese type (i.e.
372 Roquefort, Bleu d'Auvergne and Bleu de Gex). The two-step calibration approach used in the
373 present study also improved separation of spectra derived from populations 1 and 3 isolates
374 which mainly corresponded to cheese isolates from different PDO or PGI, with population 3
375 and 1 isolates originating mainly from Gorgonzola-Type cheeses and other cheeses (i.e.
376 Stilton, Cabrales, Danablu, Fourme d'ambert Bleu de Gex and Jihoceska Niva), respectively.
377 It is also worth mentioning that, as previously reported by Gillot et al. (2015), a common
378 macroscopic aspect was observed within population 3 isolates, with both a velvety to weakly
379 floccose texture and a light greenish gray to pale green color. As shown in Figure 2B, spectra
380 of several isolates from these two populations could not be clearly distinguished using MDS
381 analysis underlining the fact that they shared highly similar MS profiles and therefore
382 expressed features. The fact that spectra derived from populations 1 and 3 isolates shared
383 quite similar MS profiles may be explained by the fact that most isolates from these 2
384 populations were cheese isolates, which have been selected by cheese producers and/or by the
385 natural conditions prevailing during cheese ripening (Gillot et al. 2015). Similar results were
386 also obtained after investigating the relationship between the intraspecific variability of the
387 biological response to temperature and a_w and the different genetic populations within the
388 selected *P. roqueforti* strains (Nguyen et al. submitted).

389

390 **3.2.2 Database construction and validation**

391

392 To go further in the assessment of the MALDI-TOF MS discriminative power at the
393 intraspecific level, a database was constructed with 252 spectra, representing 42 strains, with
394 14, 15 and 13 isolates belonging to populations 1, 2 and 3, respectively. Cross-validation
395 results are shown in Table 3. Overall, the results of cross-validation showed that 94.1% of all
396 spectra (235 out of 252 spectra) were correctly assigned to their corresponding genetic
397 population. All spectra derived from population 2 and 3 isolates were either correctly
398 assigned to the right population (96.67-98.72 % of all spectra) or not identified at all (3.33-
399 1.28 % of all spectra corresponding to 3 and 1 spectra, respectively). These non-identified

400 spectra were derived from strain F41-4 from population 2 and strain F34-1 from population 3.
401 Other spectra derived from these strains were correctly assigned to their respective genetic
402 population. Identification performances of spectra derived from population 1 isolates were
403 lower than those obtained with the other two populations with 84.52% of spectra (71 out of
404 84 spectra) correctly assigned. The two spectra which yielded low discrimination results
405 corresponded to two spectra of strain F84, that were either attributed to population 1 and 3
406 while other spectra of this strain were correctly identified. One of the two unidentified spectra
407 with no identification results corresponded to one spectrum of strain F21-1, for which the
408 other five spectra were correctly assigned. The second one corresponded to one spectrum of
409 strain F81, for which three other spectra yielded discordant results as they were attributed to
410 population 3, while the last two were correctly assigned to population 1. Finally, the six
411 incorrectly assigned spectra belonged to strain F77-1 for which all spectra were incorrectly
412 assigned to population 2. This result could be explained by the fact that this isolate had MS
413 spectra which were more similar to those of several population 2 isolates (Figure 2B).
414 For external validation, 126 spectra corresponding to 21 independent isolates including 7
415 isolates from each genetic population, were used to challenge the database. The results are
416 shown in Table 4. 95.24 % of all spectra (110 out of 126 spectra) were correctly assigned to
417 their corresponding population. Spectra acquired from external isolates from populations 1
418 and 2 were all correctly assigned, with the exception of one spectrum from the strain
419 IHEM3196 and F53 from population 1 and two spectra from strain LCP03969 from
420 population 2. Finally, for external isolates from population 3, 71.43% of spectra (30 out of 42
421 spectra) were accurately assigned to their respective population. All incorrectly assigned
422 spectra (either yielding no or discordant identification) belonged to strains F28-3 and
423 UBOCC-A-101449. For strain F28-3, five out of six spectra were not identified, and the last
424 one was incorrectly attributed to population 2 while for strain UBOCC-A-101449, three out
425 of six spectra were incorrectly identified to population 1 and the other three were assigned to
426 both populations 1 and 2 by the algorithm. Interestingly, when looking in details at the allelic
427 profiles of strains F28-3 and UBOCC-A-101449, we observed that the 2 strains, despite being
428 classified in population 3 by Gillot et al. (2015), shared 1 similar allele with that of isolates
429 from population 2 and 1, respectively. Hence, it could explain why their assignment to the
430 right population was problematic.

431 Noteworthy, several strains from populations 1 and 2 that were chosen for external validation
432 also shared common alleles with isolates from other populations (Gillot et al. 2015). Indeed,
433 strains IHEM3196 and F53, that were assigned to population 1 by Gillot et al. (2015), also

434 shared 1 common allele with isolates from population 2, while strains UBOCC-A-111178,
435 DSMZ1999 and UBOCC-A-111170, assigned to population 2 by Gillot et al. (2015) shared 2
436 common alleles with population 2 and for the two other alleles, presented alleles that were
437 different from those of other isolates from population 3. Nevertheless, spectra of these
438 isolates were correctly assigned after external validation suggesting that their MS peak
439 profiles were much more closely related to that of the isolates which were used to build the
440 database.

441 As indicated in the ‘Materials and methods’ section, for database construction, peak lists of
442 spectra from each population were binned and a predictive model was established. In order to
443 understand what were the main differences in the MS spectra of the three *P. roqueforti*
444 populations, we investigated which bins (or mass-intervals) had a high impact (positive or
445 negative) for population assignment. The two bins that had the higher and lower impact on
446 population assignment are shown in Table 5. All these bins had masses ranging from 3000 to
447 7716.1 Da. In comparison, Hettick et al. (2008) found differences between spectra of
448 *Aspergillus flavus* isolates in a mass range from 7000 to 10000 Da, but in contrast to the
449 present study in which the ASC algorithm was used, such comparison was performed on
450 whole spectra based on peak lists. It is also interesting to note that high-impact weights for
451 population 2 were slightly higher than those of the two other populations and that overall,
452 high-impact bins were different depending on the population, except for the [3000.0;3004.0]
453 bin which allowed to discriminate population 3 isolates from population 1 and 2 isolates
454 (Table 5). Thus, it would be of great interest to look closer into the different bins that allowed
455 population separation during MALDI-TOF MS analysis, especially those which were
456 identified by the algorithm as having a high-impact weight. The application of MALDI-TOF
457 MS/MS could help to determine the exact m/z of proteins which allowed to discriminate *P.*
458 *roqueforti* isolates at the population level as performed previously by Freimoser et al. (2016)
459 on different *Monilinia* species. Then, after comparison with theoretical masses of proteins
460 predicted from available sequenced genomes of *P. roqueforti*, it may be possible to identify
461 which are the proteins (and their functions) that permit to discriminate one population from
462 another. However, such comparison can lead to the identification of several different proteins
463 for one single peak because different proteins can share the same m/z value (Spinali et al.
464 2015).

465 Altogether, these results suggest that there is a very good agreement between genetic data and
466 MS peak profiles and that MALDI-TOF MS could be used as a rapid tool for typing of *P.*
467 *roqueforti* isolates using a dataset of well characterized isolates at the intraspecific level.

468 Indeed, MALDI-TOF MS was able to highlight intra-specific polymorphism and yielded
469 similar results to those obtained from genetic analysis based on the study of three
470 microsatellites markers of *Penicillium roqueforti* isolates. In addition, it was even possible to
471 assign external isolates to the right populations by constructing a spectral database. However,
472 two strains which possessed allelic profiles found in other genetic populations, could not be
473 classified accurately with the approach used in the present study. Despite a very good
474 agreement between genetic data and MS profiles, it must be noted that differentiation
475 between the three populations is not made on the same markers in each analysis. Indeed,
476 genetic analysis is based on microsatellite markers, short and repeated DNA sequences
477 (Mathimaran et al. 2008), while MALDI-TOF MS detects predominantly ribosomal proteins
478 and other proteins, that are constantly expressed and highly abundant (Santos et al. 2010).

479

480 In conclusion, the results obtained in this study, together with those previously published by
481 Quero et al. (2018) confirm that MALDI-TOF MS can be a powerful tool to differentiate and
482 identify food-related filamentous fungi not only at the species level but can also be applied to
483 differentiate species complex and cryptic species as well populations from a same species.
484 This method could be of great interest for the management of mycological safety and quality
485 of foods. Indeed, correct species identification of moulds is of high importance and the
486 possibility of going beyond species identification could also be a valuable asset for source
487 tracking of fungi in the food chain.

488

489 **Acknowledgements**

490 This work was done as part of a CIFRE PhD funded by bioMérieux and the French
491 Association for Research and Technology (ANRT) [Convention #2015/0821] in collaboration
492 with the LUBEM laboratory.

493

494 **Conflict of interest**

495 LQ, PC, BC and VG are employees of bioMérieux, a company developing and selling *in vitro*
496 diagnostic assays including the VITEK MS used in this study.

497

498

499 **References**

- 500 Alanio, A., Beretti, J. -L., Dauphin, B., Mellado, E., Quesne, G., Lacroix, C., Amara, A.,
501 Berche, P., Nassif, X., Bougnoux M. -E. 2011. Matrix-assisted Laser Desorption Ionization
502 Time-of-flight Mass Spectrometry for Fast and Accurate Identification of Clinically Relevant
503 *Aspergillus* Species. Clin. Microbiol. Infec. 17, 750–755. [https://doi.org/10.1111/j.1469-](https://doi.org/10.1111/j.1469-0691.2010.03323.x)
504 0691.2010.03323.x.
- 505
506 Al-Hatmi, A.M.S., Normand, A-C, van Diepeningen, A. D., Hendrickx M., de Hoog S.G.,
507 and Renaud Piarroux. 2015. Rapid Identification of Clinical Members of *Fusarium Fujikuroi*
508 Complex Using MALDI-TOF MS. Fut. Microbiol. 10, 1939–1952.
509 <https://doi.org/10.2217/fmb.15.108>.
- 510
511 Allen, C., Prior, P., Hayward A. C. 2005. Bacterial Wilt Disease and the *Ralstonia*
512 *Solanacearum* Species Complex. American Phytopathological Society, St. Paul.
- 513
514 Bader, O. 2013. MALDI-TOF-MS-Based Species Identification and Typing Approaches in
515 Medical Mycology. Proteomics 13, 788–799. <https://doi.org/10.1002/pmic.201200468>.
- 516
517 Balasundaram, S. V., Engh I. B., Skrede I., Kausrud H. 2015. How Many DNA Markers Are
518 Needed to Reveal Cryptic Fungal Species? Fung. Biol. 119, 940–45.
519 <https://doi.org/10.1016/j.funbio.2015.07.006>.
- 520
521 Basile, F., Beverly, M.B., Voorhees K. J., Hadfield T. L. 1998. Pathogenic Bacteria: Their
522 Detection and Differentiation by Rapid Lipid Profiling with Pyrolysis Mass Spectrometry.
523 Trac-Trends Anal. Chem. 117, 95–109. [https://doi.org/10.1016/S0165-9936\(97\)00103-9](https://doi.org/10.1016/S0165-9936(97)00103-9).
- 524
525 Belén Flórez, A, Álvarez-Martín, P., López-Díaz, T.M., Mayo, B. 2007. Morphotypic and
526 Molecular Identification of Filamentous Fungi from Spanish Blue-Veined Cabrales Cheese,
527 and Typing of *Penicillium Roqueforti* and *Geotrichum Candidum* Isolates. Int. Dairy J. 17,
528 350–357. <https://doi.org/10.1016/j.idairyj.2006.04.002>.
- 529
530 Carvajal-Campos, A., Manizan, A.L., Tadrist, S., Akaki, D. K., Koffi-Nevry, R., Moore,
531 G.G., Fapohunda, S.O., et al. 2017. *Aspergillus korhogoensis*, a Novel Aflatoxin Producing
532 Species from the Côte d’Ivoire. Toxins 9, e353. <https://doi.org/10.3390/toxins9110353>.
- 533

534 De Carolis, E., Vella, A., Florio, A. R, Posteraro, P., Perlin, D. S., Sanguinetti, M., and
535 Posteraro B.. 2012. Use of Matrix-Assisted Laser Desorption Ionization-Time of Flight Mass
536 Spectrometry for Caspofungin Susceptibility Testing of *Candida* and *Aspergillus* Species. J.
537 Clin. Microbiol. 50, 2479–2483. <https://doi.org/10.1128/JCM.00224-12>.

538

539 Deak, E., Charlton, C. L., Bobenchik, A. M., Miller, S. A., Pollett, S., McHardy, I. H., Wu,
540 M. T., Garner, O. B.. 2015. Comparison of the Vitek MS and Bruker Microflex LT MALDI-
541 TOF MS Platforms for Routine Identification of Commonly Isolated Bacteria and Yeast in
542 the Clinical Microbiology Laboratory. Diagn. Microbiol. Infect. Dis. 81, 27–33.
543 <https://doi.org/10.1016/j.diagmicrobio.2014.09.018>.

544

545 Filtenborg, O., J. C. Frisvad, and U. Thrane. 1996. Moulds in Food Spoilage. Int. J. Food
546 Microbiol. 33, 85–102. [https://doi.org/10.1016/0168-1605\(96\)01153-1](https://doi.org/10.1016/0168-1605(96)01153-1).

547

548 Fontaine, K., Hymery N., Lacroix M. Z., Puel S., Puel O., Rigalma, K., Gaydou, V., Coton, E.,
549 Mounier, J. 2015. Influence of Intraspecific Variability and Abiotic Factors on Mycotoxin
550 Production in *Penicillium Roqueforti*. Int. J. Food Microbiol. 215, 187–193.
551 <https://doi.org/10.1016/j.ijfoodmicro.2015.07.021>.

552

553 Freimoser, F. M., Hilber-Bodmer, M., Brunisholz, R., Drissner D. 2016. Direct Identification
554 of *Monilinia* Brown Rot Fungi on Infected Fruits by Matrix-Assisted Laser
555 Desorption/Ionization (MALDI) Mass Spectrometry. Chem. Biol. Technol. Agric. 3, 7.
556 <https://doi.org/10.1186/s40538-016-0058-4>.

557

558 Frisvad, J. C., Hubka, V., Ezekiel, C. N., Hong, S. -B, Nováková, A., Chen, A. J, Arzanlou,
559 M., et al. 2019. Taxonomy of *Aspergillus* Section *Flavi* and Their Production of Aflatoxins,
560 Ochratoxins and Other Mycotoxins. Stud. Mycol. 93, 1–63.
561 <https://doi.org/10.1016/j.simyco.2018.06.001>.

562

563 Fujinami, Y., Kikkawa, H. S., Kurosaki, Y., Sakurada, K., Yoshino, M., and Yasuda, J. 2011.
564 Rapid Discrimination of *Legionella* by Matrix-Assisted Laser Desorption Ionization Time-of-
565 Flight Mass Spectrometry. Microbiol. Res. 166, 77–86.
566 <https://doi.org/10.1016/j.micres.2010.02.005>.

567

568 Gibbons, J. G., Salichos, L., Slot J. C., Rinker, D. C., McGary, K. L., King, J. G. Klich, M.
569 A., Tabb, D. L., McDonald, W. Hayes, Rokas A.. 2012. The Evolutionary Imprint of
570 Domestication on Genome Variation and Function of the Filamentous Fungus *Aspergillus*
571 *oryzae*. *Curr. Biol.* 22, 1403–1409. <https://doi.org/10.1016/j.cub.2012.05.033>.

572

573 Gillot, G., Jany J-L., Coton, M., Le Floch, G., Debaets, S., Ropars J., López-Villavicencio,
574 M., et al. 2015. Insights into *Penicillium roqueforti* Morphological and Genetic Diversity.
575 *PLoS One* 10, e0129849. <https://doi.org/10.1371/journal.pone.0129849>.

576

577 Girard, V., Mailler, S., Welker, M., Arzac, M., Cellière, B., Cotte-Pattat, P-J., Chatellier,
578 S., et al. 2016. Identification of *Mycobacterium* Spp. and *Nocardia* Spp. from Solid and
579 Liquid Cultures by Matrix-Assisted Laser Desorption Ionization–time of Flight Mass
580 Spectrometry (MALDI-TOF MS). *Diagn. Microbiol. Infect. Dis.* 86, 277–283.
581 <https://doi.org/10.1016/j.diagmicrobio.2016.07.027>.

582

583 Hawksworth, D.L. 2006. Pandora’s Mycological Box: Molecular Sequences vs. Morphology
584 in Understanding Fungal Relationships and Biodiversity. *Rev. Iberoam. Micol.* 23, 127–133.

585

586 Hettick, J. M., Green, B. J., Buskirk, A. D., Kashon, M. L., Slaven J. E., Janotka, E.,
587 Blachere, F. M., Schmechel, D., Beezhold D.H.. 2008. Discrimination of *Aspergillus* Isolates
588 at the Species and Strain Level by Matrix-Assisted Laser Desorption/Ionization Time-of-
589 Flight Mass Spectrometry Fingerprinting. *Anal. Biochem.* 380, 276–281.
590 <https://doi.org/10.1016/j.ab.2008.05.051>.

591

592 Imbert, S., Normand, A.C., Gabriel, F., Cassaing, S., Bonnal, C., Costa, D., Lachaud, L.,
593 Hasseine, L., Kristensen, L., Schuttler, C., Raberin, H., Brun, S., Hendrickx, M., Stubbe, D.,
594 Piarroux, R., Fekkar, A.. 2019. Multi-centric evaluation of the online MSI platform for the
595 identification of cryptic and rare species of *Aspergillus* by MALDI-TOF. *Med. Mycol.*
596 <https://doi.org/10.1093/mmy/myz004>.

597

598 Kern, C. C., Vogel, R. F., Behr, J.. 2014. Differentiation of *Lactobacillus brevis* Strains
599 Using Matrix-Assisted-Laser-Desorption-Ionization-Time-of-Flight Mass Spectrometry with
600 Respect to Their Beer Spoilage Potential. *Food Microbiol.* 40, 18–24.
601 <https://doi.org/10.1016/j.fm.2013.11.015>.

602

603 Kuhns, M., Zautner, A. E., Rabsch, W., Zimmermann, O., Weig, M., Bader, O., Groß, U..
604 2012. Rapid Discrimination of Salmonella Enterica Serovar Typhi from Other Serovars by
605 MALDI-TOF Mass Spectrometry. PloS One 7, e40004.
606 <https://doi.org/10.1371/journal.pone.0040004>.

607
608 Lauterbach, A., Usbeck, J. C., Behr, J., Vogel, R. F. 2017. MALDI-TOF MS Typing Enables
609 the Classification of Brewing Yeasts of the Genus *Saccharomyces* to Major Beer Styles. PloS
610 One 12, e0181694. <https://doi.org/10.1371/journal.pone.0181694>.

611
612 Li, Y., Wang, H., Zhao Y-P., Xu Y-C., Hsueh P-R. 2017. Evaluation of the Bruker Biotyper
613 Matrix-Assisted Laser Desorption/Ionization Time-of-Flight Mass Spectrometry System for
614 Identification of *Aspergillus* Species Directly from Growth on Solid Agar Media. Front
615 Microbiol 8, 1209. <https://doi.org/10.3389/fmicb.2017.01209>.

616
617 Masih, A., Singh, P. K., Kathuria, S., Agarwal, K., Meis, J. F., Chowdhary, A. 2016.
618 Identification by Molecular Methods and Matrix-Assisted Laser Desorption Ionization–Time
619 of Flight Mass Spectrometry and Antifungal Susceptibility Profiles of Clinically Significant
620 Rare *Aspergillus* Species in a Referral Chest Hospital in Delhi, India. J. Clin. Microbiol. 54,
621 2354–64. <https://doi.org/10.1128/JCM.00962-16>.

622
623 Mathimaran, N., Falquet, L., Ineichen, K., Picard, C., Redecker, D., Boller, T., Wiemken A.
624 2008. Microsatellites for Disentangling Underground Networks: Strain-Specific Identification
625 of *Glomus* Intraradices, an Arbuscular Mycorrhizal Fungus.
626 Fungal Genet. Biol. 45, 812–17. <https://doi.org/10.1016/j.fgb.2008.02.009>.

627
628 Normand, A.C., Cassagne, C., Ranque, S., L'Ollivier, C., Fourquet, P., Roesems, S.,
629 Hendrickx, M., Piarroux, R. 2013. Assessment of various parameters to improve MALDI-
630 TOF MS reference spectra libraries constructed for the routine identification of filamentous
631 fungi. BMC Microbiol. 13:76. <https://doi.org/10.1186/1471-2180-13-76>.

632
633 Park, J. H., Shin, J. H., Choi, M. J., Choi, J. U., Park, Y. J., Jang, S. J., Won, E. J., et al. 2017.
634 Evaluation of Matrix-Assisted Laser Desorption/Ionization Time-of-Fight Mass Spectrometry
635 for Identification of 345 Clinical Isolates of *Aspergillus* Species from 11 Korean Hospitals:
636 Comparison with Molecular Identification. Diagn. Microbiol. Infect. Dis. 87, 28–31.
637 <https://doi.org/10.1016/j.diagmicrobio.2016.10.012>.

638

639 Pitt, J., and Hocking, A. 2009. Fungi and Food Spoilage. 3rd ed. Springer Science &
640 Business media, New York.

641

642 Pulcrano, G., Roscetto, E., Iula, V. D., Panellis, D., Rossano, F., Catania. M. R. 2012.
643 MALDI-TOF Mass Spectrometry and Microsatellite Markers to Evaluate *Candida*
644 *Parapsilosis* Transmission in Neonatal Intensive Care Units. Eur. J. Clin. Microbiol. Infect.
645 Dis. 31, 2919–2928. <https://doi.org/10.1007/s10096-012-1642-6>.

646

647 Laura Q., Girard V., Pawtowski A., Tréguer, S., Weill A., Arend S., Cellière, B., Polsinelli,
648 S., Monnin, V., Van Belkum, A., Vasseur, V., Nodet, P., Mounier, J.. 2018. Development and
649 Application of MALDI-TOF MS for Identification of Food Spoilage Fungi. Food Microbiol.
650 (in press). <https://doi.org/10.1016/j.fm.2018.05.001>.

651

652 Rodrigues, P., Santos, C., Venâncio, A., Lima, N. 2011. Species Identification of *Aspergillus*
653 Section *Flavi* Isolates from Portuguese Almonds Using Phenotypic, Including MALDI-TOF
654 ICMS, and Molecular Approaches. J. Appl. Microbiol. 111, 877–892.
655 <https://doi.org/10.1111/j.1365-2672.2011.05116.x>.

656

657 Ropars, J., López-Villavicencio, M., Dupont, J., Snirc, A., Gillot, G., Coton, M., Jany, J-L.,
658 Coton, E., Giraud, T.. 2014. Induction of Sexual Reproduction and Genetic Diversity in the
659 Cheese Fungus *Penicillium Roqueforti*. Evol. Appl. 7, 433–441.
660 <https://doi.org/10.1111/eva.12140>.

661

662 Santos, C., Paterson, R. R. M., Venâncio, A., Lima, N. 2010. Filamentous Fungal
663 Characterizations by Matrix-Assisted Laser Desorption/Ionization Time-of-Flight Mass
664 Spectrometry. J. Appl. Microbiol. 108, 375–385. [https://doi.org/10.1111/j.1365-](https://doi.org/10.1111/j.1365-2672.2009.04448.x)
665 [2672.2009.04448.x](https://doi.org/10.1111/j.1365-2672.2009.04448.x).

666

667 Soares, C., Rodrigues, P., Peterson, S.W., Lima, N., Venâncio, A. 2012. Three new species of
668 *Aspergillus* section *Flavi* isolated from almonds and maize in Portugal. Mycologia 104, 682–
669 697.

670

671 Spinali, S., van Belkum, A., Goering, R. V., Girard, V., Welker, M., Van Nuenen, M.,
672 Pincus, D. H., Arsac, M., Durand, G. 2015. Microbial Typing by Matrix-Assisted Laser
673 Desorption Ionization-Time of Flight Mass Spectrometry: Do We Need Guidance for Data
674 Interpretation? J. Clin. Microbiol. 53, 760–765. <https://doi.org/10.1128/JCM.01635-14>.

675
676 Tam, E. W. T., Chen, J. H. K., Lau, E. C. L., Ngan, Antonio H. Y., Fung, K. S. C. Lee, K-C.,
677 Lam, C-W., Yuen K-Y., Lau, S. K. P., Woo, P. C. Y. 2014. Misidentification of *Aspergillus*
678 *nomius* and *Aspergillus tamarii* as *Aspergillus flavus*: Characterization by Internal
679 Transcribed Spacer, β -Tubulin, and Calmodulin Gene Sequencing, Metabolic Fingerprinting,
680 and Matrix-Assisted Laser Desorption Ionization-Time of Flight Mass Spectrometry. J. Clin.
681 Microbiol. 52, 1153–60. <https://doi.org/10.1128/JCM.03258-13>.

682
683 Ueda, O., Tanaka, S., Nagasawa, Z., Hanaki, H., Shobuike, T., Miyamoto, H. 2015.
684 Development of a Novel Matrix-Assisted Laser Desorption/Ionization Time-of-Flight Mass
685 Spectrum (MALDI-TOF-MS)-Based Typing Method to Identify Meticillin-Resistant
686 *Staphylococcus aureus* Clones. J. Hosp. Infect. 90, 147–155.
687 <https://doi.org/10.1016/j.jhin.2014.11.025>.

688
689 Usbeck, J. C., Wilde, C., Bertrand, D., Behr, J., Vogel, R. F. 2014. Wine Yeast Typing by
690 MALDI-TOF MS. Appl. Microbiol. Biotechnol. 98, 3737–3752.
691 <https://doi.org/10.1007/s00253-014-5586-x>.

692
693 Varga, J., Frisvad, J.C., Samson, R.A. 2019. Two new aflatoxin producing species, and an
694 overview of *Aspergillus* section *Flavi*. Stud. Mycol. 69, 57–80.

695
696 Vargha, M., Takáts, Z., Konopka, A. and Nakatsu, C. H. 2006. Optimization of MALDI-TOF
697 MS for Strain Level Differentiation of *Arthrobacter* Isolates. J. Microbiol. Methods 66, 399–
698 409. <https://doi.org/10.1016/j.mimet.2006.01.006>.

699
700 Waśkiewicz, A. 2014. MYCOTOXINS | Natural Occurrence of Mycotoxins in Food, in: Batt
701 C. A. and Tortorello M.L. (Eds.), Encyclopedia of Food Microbiology, second ed. Academic
702 Press, Oxford, pp. 880–886. <https://doi.org/10.1016/B978-0-12-384730-0.00231-7>.

703
704 Welham, K. J., Domin, M. A., Johnson, K., Jones, L., Ashton, D. S. 2000. Characterization of
705 Fungal Spores by Laser Desorption/Ionization Time-of-Flight Mass Spectrometry. Rapid
706 Commun. Mass Spectrom. 14, 307–310. [https://doi.org/10.1002/\(SICI\)1097-](https://doi.org/10.1002/(SICI)1097-0231(20000315)14:5<307::AID-RCM823>3.0.CO;2-3)
707 [0231\(20000315\)14:5<307::AID-RCM823>3.0.CO;2-3](https://doi.org/10.1002/(SICI)1097-0231(20000315)14:5<307::AID-RCM823>3.0.CO;2-3).

708 Table 1. *Aspergillus* spp. isolates from *Aspergillus* section *Flavi* analyzed by MALDI-TOF MS in the
 709 present study.

Clade	Species	Strain number	Origin substrate
<i>Avenaceus</i>	<i>Aspergillus avenaceus</i>	NRRL 517 ^T	Green pea
		NRRL 4517	Unknown
<i>Bertholletius</i>	<i>Aspergillus bertholletius</i>	CCT 7615 ^T	Rain forest soil
<i>Coremiiformis</i>	<i>Aspergillus coremiiformis</i>	NRRL 13603 ^T	Soil
<i>Flavus</i>	<i>Aspergillus aflatoxiformans</i> (<i>ex A. parvisclerotigenus</i>)	CBS 121.62	<i>Arachis hypogea</i>
		SF1	Rain forest soil
		SF6	Rain forest soil
<i>Flavus</i>	<i>Aspergillus arachidicola</i>	UBOCC-A-117374 = CBS 117612	<i>Arachis glabrata</i> leaf
		UBOCC-A-117375 = CBS 117611	<i>Arachis glabrata</i> leaf
		UBOCC-A-117376 = CBS 117614	<i>Arachis glabrata</i> leaf
		UBOCC-A-117377 = CBS 117615	<i>Arachis glabrata</i> leaf
		UBOCC-A-117373 = CBS 117610 ^T	<i>Arachis glabrata</i> leaf
<i>Flavus</i>	<i>Aspergillus cerealis</i> (<i>ex A. korhogoensis</i>)	NRRL 66708 = MACI46	Peanut pods
<i>Flavus</i>	<i>Aspergillus flavus</i>	UBOCC-A-108068 = LCP 89.4253	Molten cheese
		UBOCC-A-108067 = CBS 100927 ^T	Cellophane
		UBOCC-A-101061	Pig feed
		UBOCC-A-101063	Cotton oil cake
		UBOCC-A-106028	Wheat
		UBOCC-A-106029	Pig feed
		UBOCC-A-106030	Wheat
		UBOCC-A-106031	Maize
		UBOCC-A-106032	Barley
UBOCC-A-106033	Poultry feed		
<i>Flavus</i>	<i>Aspergillus minisclerotigenes</i>	UBOCC-A-117303 = CBS 117635 ^T	<i>Arachis hypogea</i> seed
		UBOCC-A-117304 = CBS 117633	<i>Arachis hypogea</i> seed
		UBOCC-A-117305 = CBS 117634	<i>Arachis hypogea</i> seed
		UBOCC-A-117306 = CBS 117620	<i>Arachis hypogea</i> seed
		UBOCC-A-117307 = CBS 117639	<i>Arachis hypogea</i> seed
		NRRL 29000	Peanut soil
<i>Flavus</i>	<i>Aspergillus mottae</i>	MUM 10.231 ^T	Maize kernel
<i>Flavus</i>	<i>Aspergillus novoparasiticus</i>	AFc32 = NRRL 62795	Cassava
		UBOCC-A-117379 = CBS 126850	Air sample
		UBOCC-A-117378 = CBS 126849 ^T	Human sputum
		LEMI 267	Human sputum
<i>Flavus</i>	<i>Aspergillus oryzae</i>	CBS 100925 ^T	Unknown
<i>Flavus</i>	<i>Aspergillus parasiticus</i>	UBOCC-A-111038 = CBS 100308	Unknown
		UBOCC-A-111039	Unknown
		UBOCC-A-111041 = CBS 971.97	Indian sweets
		UBOCC-A-110223 = CBS 100926 ^T	Sugar cane mealy bug
		NRRL 492	Unknown

<i>Flavus</i>	<i>Aspergillus sergii</i>	MUM 10.219 ^T MUM 10.251	Prune fruit Almond shell
<i>Flavus</i>	<i>Aspergillus sojae</i>	CBS 134.52 CBS 100928 ^T	Soy sauce Soy sauce
<i>Flavus</i>	<i>Aspergillus transmontanensis</i>	MUM 10.205 MUM 10.214 ^T	Almond Almond
<i>Leporis</i>	<i>Aspergillus leporis</i>	NRRL 3216 ^T NRRL 6599	Dung of <i>Lepus townsensii</i> Soil
<i>Nomius</i>	<i>Aspergillus luteovirescens</i> (ex <i>A bombycis</i>)	NRRL 25010 NRRL 25593	Frass in silkworm house Frass in silkworm house
<i>Nomius</i>	<i>Aspergillus nomius</i>	CBS 123901 NRRL 13137 ^T NRRL 6552	Keratitis Wheat Pine sawfly
<i>Nomius</i>	<i>Aspergillus pseudonomius</i>	NRRL 3353 ^T	Diseased alkali bee
<i>Tamarii</i>	<i>Aspergillus caelatus</i>	CBS 763.97 ^T NRRL 25568	Soil Soil
<i>Tamarii</i>	<i>Aspergillus pseudocaelatus</i>	CBS 117616 ^T	<i>Arachis burkartii</i> leaf
<i>Tamarii</i>	<i>Aspergillus pseudotamarii</i>	CBS 766.97 ^T CBS 117628 NRRL 443 NRRL 25518	Teafield soil Teafield soil Unknown Teafield soil
<i>Tamarii</i>	<i>Aspergillus tamarii</i>	UBOCC-A-110176 = CBS 104.13 ^T UBOCC-A-110179 = CBS 104.14 UBOCC-A-110219 = CBS 129.49 UBOCC-A-110225 = CBS 590.68 UBOCC-A-111043 UBOCC-A-111045 UBOCC-A-111046	Charcoal Tomato Coffee tree seed Nutmeg Charcoal Coffee tree seed Nutmeg

710 ^TType strain

711 UBOCC, Université de Bretagne Occidentale Culture Collection ; CBS, Centraalbureau voor

712 Schimmelcultures Collection ; MUM, Micoteca da Universidad do Minho ; NRRL, National Center

713 for Agricultural Utilization Research

714

715

716

717 Table 2. Identification performances of *Aspergillus* section *Flavi* species after cross-
 718 validation.

Species	Overall correct	Single choice	Low discrimination	No identification	Discordant
<i>A. aflatoxiformans</i>	100% (11/11)*	100% (11/11)	0% (0/11)	0% (0/11)	0% (0/11)
<i>A. arachidicola</i>	100% (18/18)	100% (18/18)	0% (0/18)	0% (0/18)	0% (0/18)
<i>A. avenaceus</i>	100% (10/10)	90% (9/10)	10% (1/10)	0% (0/10)	0% (0/10)
<i>A. luteovirescens</i>	100% (12/12)	100% (12/12)	0% (0/12)	0% (0/12)	0% (0/12)
<i>A. caelatus</i>	100% (12/12)	100% (12/12)	0% (0/12)	0% (0/12)	0% (0/12)
<i>A. flavus</i>	100% (38/38)	100% (38/38)	0% (0/38)	0% (0/38)	0% (0/38)
<i>A. leporis</i>	100% (12/12)	100% (12/12)	0% (0/12)	0% (0/12)	0% (0/12)
<i>A. minisclerotigenes</i>	100% (25/25)	100% (25/25)	0% (0/25)	0% (0/25)	0% (0/25)
<i>A. nomius</i>	100% (12/12)	100% (12/12)	0% (0/12)	0% (0/12)	0% (0/12)
<i>A. novoparasiticus</i>	95% (19/20)	95% (19/20)	0% (0/20)	5% (1/20)	0% (0/20)
<i>A. parasiticus</i>	100% (20/20)	100% (20/20)	0% (20/20)	0% (20/20)	0% (20/20)
<i>A. pseudotamarii</i>	100% (24/24)	100% (24/24)	0% (0/24)	0% (0/24)	0% (0/24)
<i>A. sergii</i>	100% (11/11)	100% (11/11)	0% (0/11)	0% (0/11)	0% (0/11)
<i>A. sojae</i>	100% (12/12)	100% (12/12)	0% (0/12)	0% (0/12)	0% (0/12)
<i>A. tamarii</i>	100% (26/26)	100% (26/26)	0% (0/26)	0% (0/26)	0% (0/26)
<i>A. transmontanensis</i>	100% (9/9)	100% (9/9)	0% (0/9)	0% (0/9)	0% (0/9)
Global performances	99.65% (271/272)	99.3% (270/272)	0.35% (1/272)	0.35% (1/272)	0% (0/272)

*number of spectra out of the total number of spectra acquired

719
720

721 Table 3. Classification performance of *P. roqueforti* isolates into three genetic populations
 722 after cross-validation.

Population	Overall correct	Single choice	Low discrimination	No identification	Discordant
1	86.9 % (73/84)*	84.52% (71/84)	2.38% (2/84)	2.38% (2/84)	10.71% (9/84)
2	96.67 % (87/90)	96.67% (87/90)	0% (0/90)	3.33% (3/90)	0% (0/90)
3	98.72 % (77/78)	98.72% (77/78)	0% (0/78)	1.28% (1/78)	0% (0/78)
Total	94.1 % (237/252)	93.3% (235/252)	0.79% (2/252)	2.33% (6/252)	3.57% (9/252)

723 *number of spectra out of the total number of spectra acquired

724

725

726

727 Table 4. Classification performance of *P. roqueforti* isolates into three genetic populations
 728 after external validation.

Population	Correct identification	No identification	Discordant
1	95.24% (40/42)*	4.76% (2/42)	0% (0/42)
2	95.24% (40/42)	2.38% (1/42)	2.38% (1/42)
3	71.43% (30/42)	11.90% (5/42)	16.67% (7/42)
Total	87.3% (110/126)	6.35% (8/126)	6.35% (8/126)

729 *number of spectra out of the total number of spectra acquired

730 Table 5. List of bins allowing classification with the ACS algorithm of *P. roqueforti* isolates
 731 into three distinct genetic population after MALDI-TOF MS analysis.

732

	High positive weight group 1	High negative weight group 1	High positive weight group 3	High negative weight group 3
High negative weight group 2	[4423.3;4429.3]* [3938.5;3943.8]		[3943.8;3949.1] [3382.8;3387.3]	
High positive weight group 2		[7208.4;7218.1] [6470.0;6478.6]		[3000;3004] [7705.8;7716.1]
High negative weight group 3	[3000.0;3004.0] [44423.3;4429.3]			
High positive weight group 3		[5410.7;5417.9] [3056.6;3060.6]		

733

734 *Mass range in Da

735

736

737

738

739

740

741

742

743

744

745

746

747

748

749

750

751

752

753

754

755

756

757 **Figure legends.**

758

759 Figure 1. (A) Multidimensional scaling (MDS) of the spectra dataset obtained after MALDI-
760 TOF MS analysis of 23 species of *Aspergillus* belonging to the *Flavi* section. Spectra are
761 colored according to the respective species to which they belong. Spectra circled in dashed-
762 red, dashed-blue and dashed green correspond to spectra of groups A, B and C, respectively.

763 (B) Multidimensional scaling (MDS) of the spectra dataset obtained after MALDI-TOF MS
764 analysis of 12 species of *Aspergillus* belonging to the *A. flavus* clade of *Flavi* section. Spectra
765 are colored according to the respective species to which they belong.

766 (C) Multidimensional scaling (MDS) of the spectra dataset obtained after MALDI-TOF MS
767 analysis of 11 species of *Aspergillus* belonging to the *A. tamarii*, *A. bertholletius*, *A. nomius*,
768 *A. coremiiformis*, *A. leporis* and *A. avenaceus* clades of *Flavi* section. Spectra are colored
769 according to the respective species to which they belong.

770

771 Figure 2. (A) Multidimensional scaling (MDS) of the spectra dataset obtained after MALDI-
772 TOF MS analysis of *P. roqueforti* isolates based on 6 replicates per strain (3 biological
773 replicates and 2 technical replicates), before calibration of the spectra. Spectra are colored
774 according to the respective genetic populations to which the isolates belong.

775 (B) Multidimensional scaling (MDS) of the spectra dataset obtained after MALDI-TOF MS
776 analysis of *P. roqueforti* isolates based on 6 replicates per strain (3 biological replicates and 2
777 technical replicates), after calibration of the spectra. Spectra are colored according to the
778 respective genetic populations to which the isolates belong. Spectra circled in dashed-green
779 and –blue correspond to spectra from *P. roqueforti* F41-4 and F77-1, respectively.

780

781

782

783

784

785

786

787

788

789

790

791

792

793

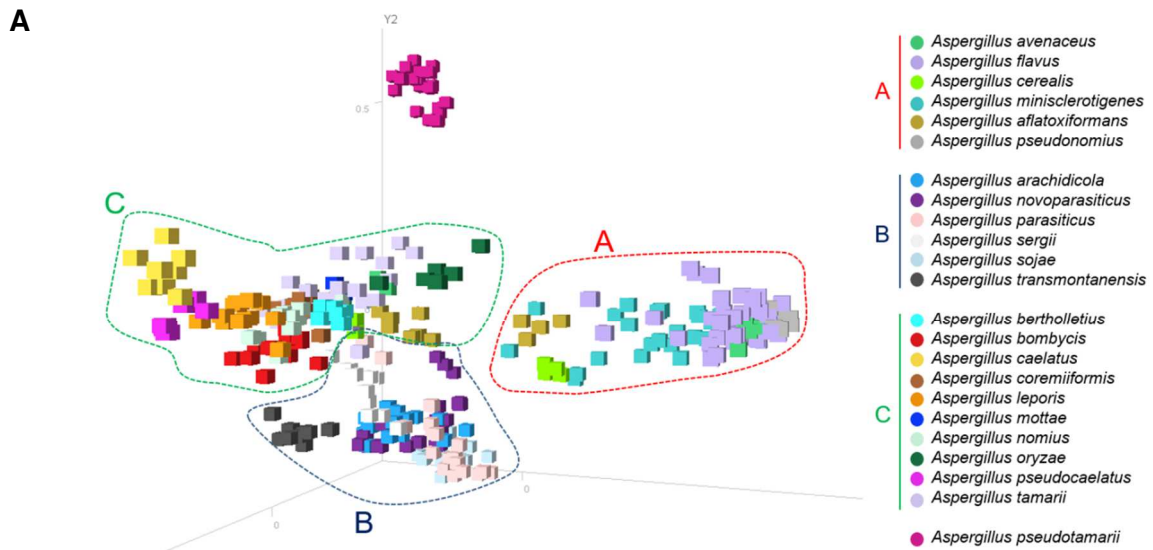
794

795

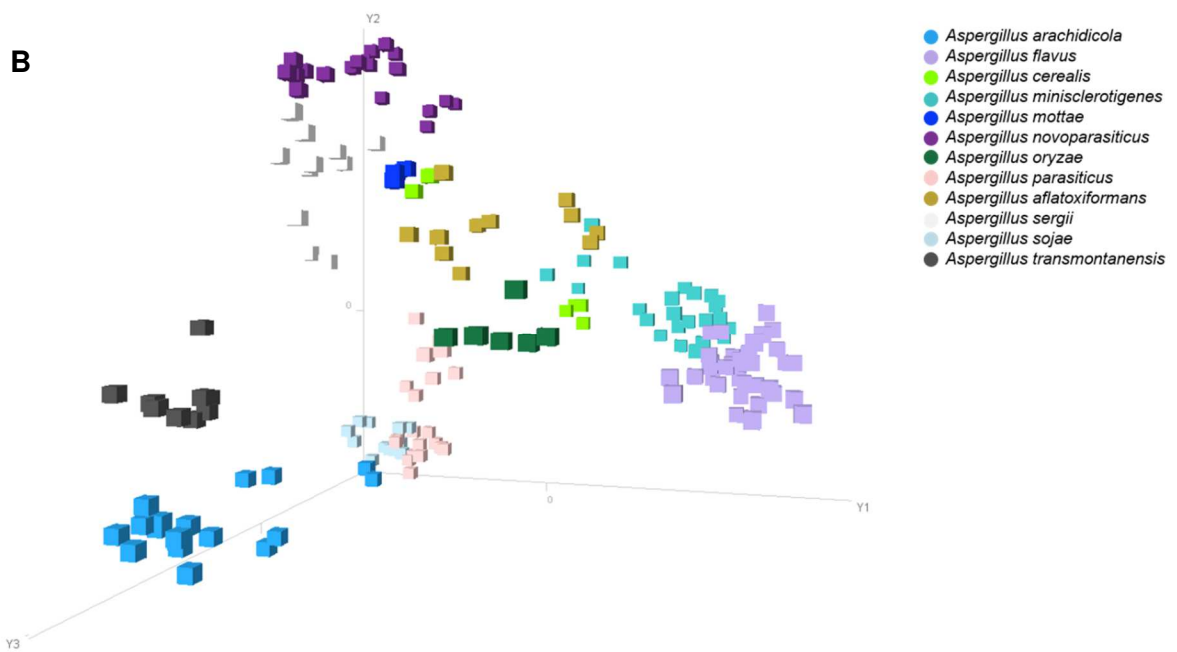
796

797 Figure 1.

798

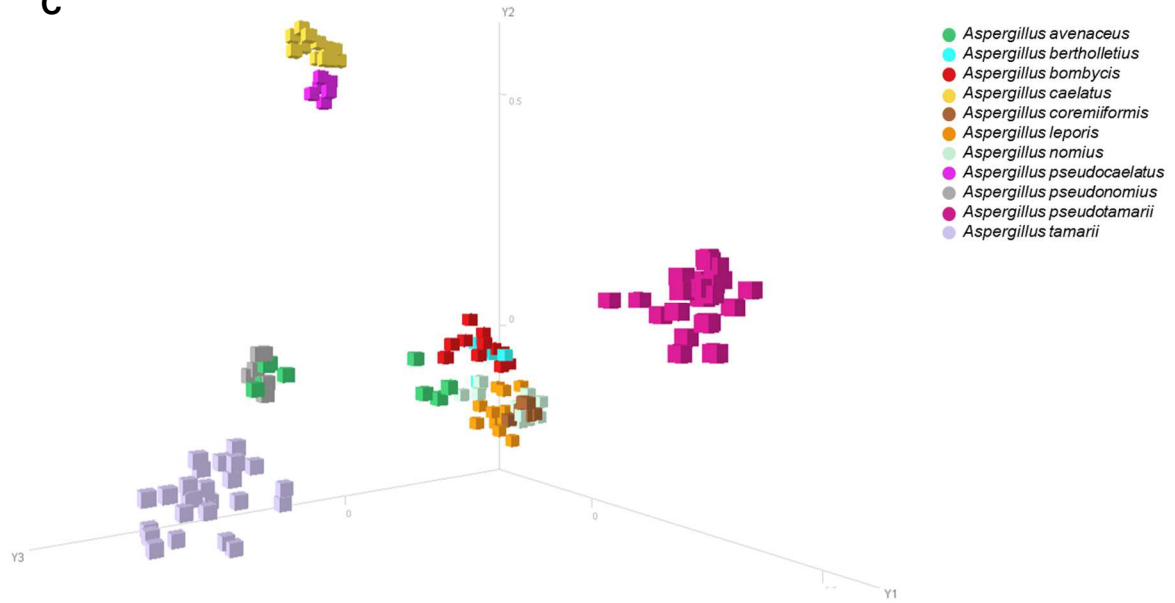


799



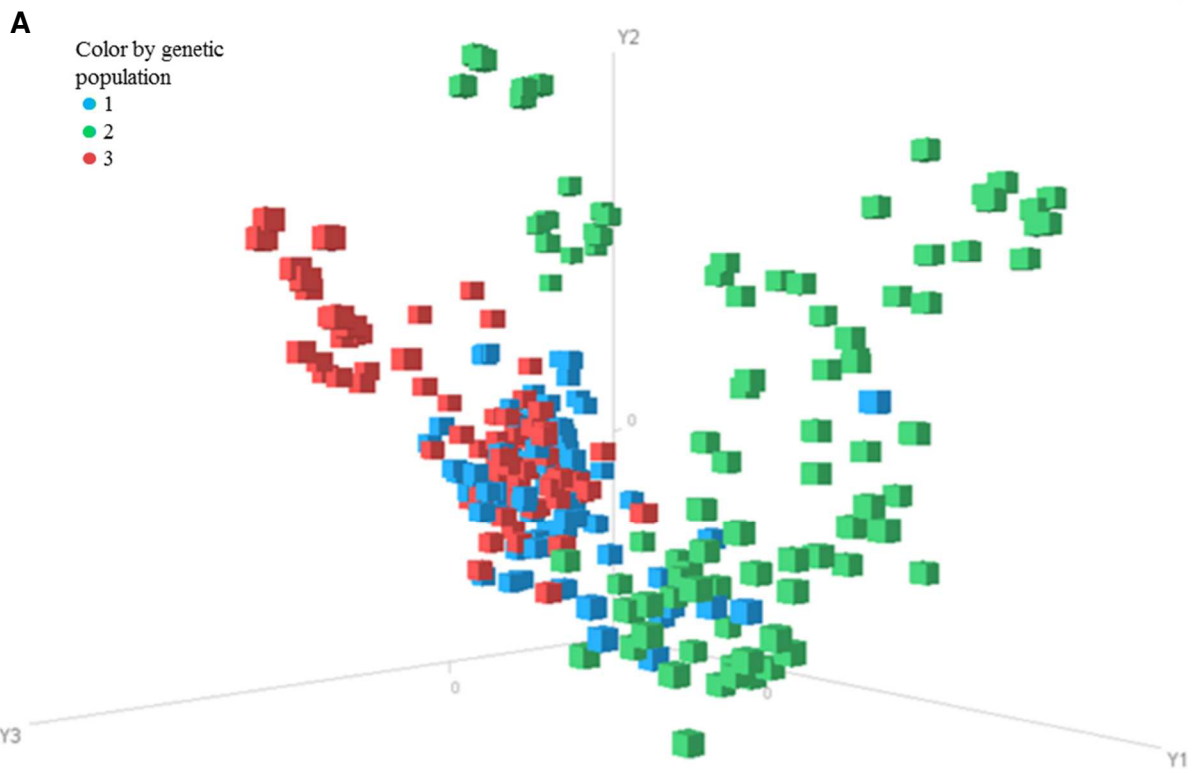
800

C

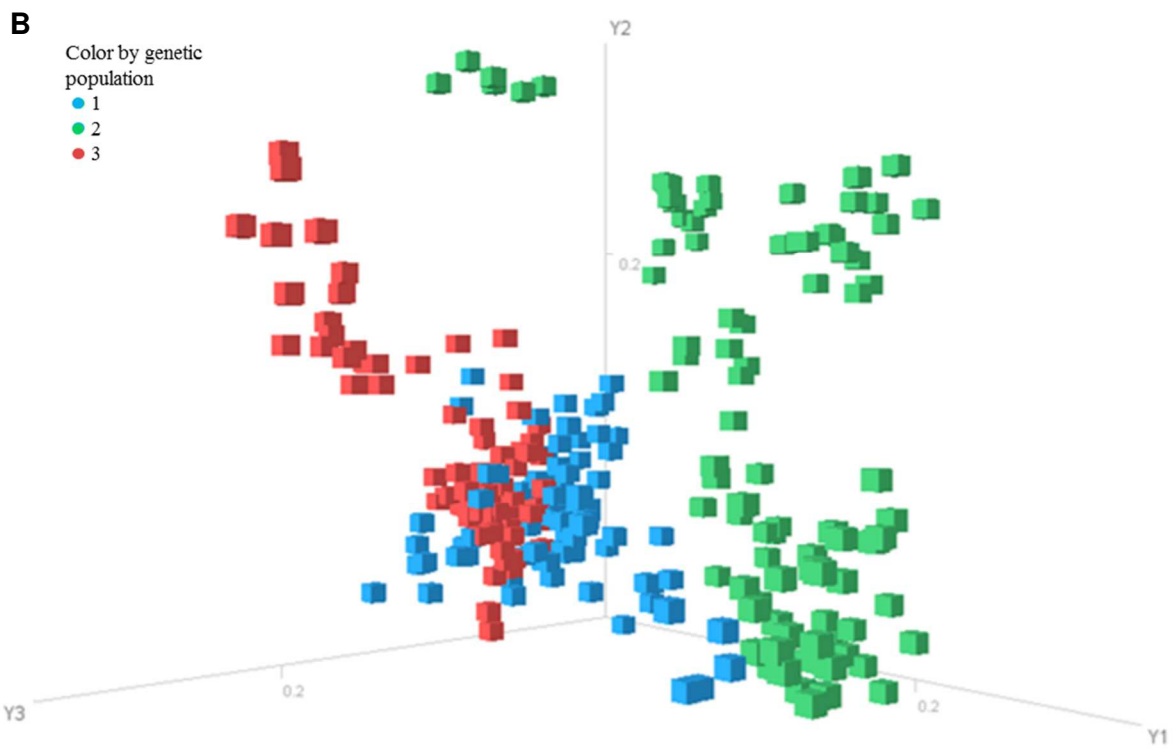


801
802
803
804
805
806
807
808
809
810
811
812
813
814
815
816
817
818
819
820
821
822
823
824
825

826 **Figure 2.**



827



828

829

830

831

832

833